Photoelectrocatalytic degradation of reactive brilliant orange K-R in a new continuous flow photoelectrocatalytic reactor

Wenbing Zhang, Taicheng An[*], Xianming Xiao, Jiamo Fu,
Guoying Sheng, Mingchao Cui, Guiying Li

*State Key Laboratory of Organic Geochemistry, Guangdong Key Laboratory of Environmental Resources Utilization and Protection,
Guangzhou Institute of Geochemistry, Chinese Academy of Sciences, Guangzhou 510640, PR China*

Abstract

A new continuous flow three-dimensional electrode-packed bed photocatalytic reactor was developed to investigate the feasibility of an electrochemically assisted photocatalytic process in the degradation of reactive brilliant orange K-R dye in $0.5\,\mathrm{mmol\,l^{-1}}$ NaCl solution. It was found that the dye could be degraded more efficiently by this photoelectrochemical process than the degradation obtained by photocatalytic oxidation or by electrochemical oxidation alone, in terms of both decolorization and TOC removal. Various parameters, such as applied cell voltage, initial concentration of chloride ion and the dye, pH value and airflow were the major factors affecting the oxidation rate of the dye. It is interesting to find that an obvious enhancement effect rather than a scavenging effect on the photoelectrocatalytic degradation of the dye in a salt solution was obtained in the new-designed photoelectrocatalytic reactor.
© 2003 Elsevier B.V. All rights reserved.

Keywords: Photoelectrocatalytic; Photocatalytic; Reactor; Dye; Wastewater

1. Introduction

Heterogeneous photocatalytic processes, especially with use of titanium dioxide, have been extensively applied in the treatment of wastewater [1,2]. Numerous studies have shown that the application of this method can lead to complete color removal, detoxification and mineralization of textile dyes wastewater [3–6]. However, owing to rapidly recombination between the photogenerated electrons and the holes, the development of a practical water treatment system relative to the photocatalytic oxidation has not been

successfully achieved yet [7]. Recently, several attempts have been made to increase the photocatalytic efficiency of titanium dioxide; these include noble metal deposition, ion doping, the addition of inorganic co-adsorbent and photoelectrochemical technology [8–11]. The photoelectrochemical technology with external potential appears promising for research on photocatalytic degradation of organic pollutants, and many academic studies have been focused on this area [12–18]. The anodic bias on TiO_2 electrode could drive away the photogenerated-electrons and -holes in different directions, and would reduce their recombination; thus, it would accelerate the oxidation of organic materials. However, most studies on electrochemically assisted photocatalysis are just to present a proof-of-concept. Few researches concerning the

* Corresponding author. Tel.: +86-20-8529-0180;
fax: +86-20-8529-0706.
E-mail address: antc99@gig.ac.cn (T. An).

photoelectrochemical reactor have been reported [9,19].

More recently, our research group has successfully combined the slurry photocatalytic oxidation technology with plate electrodes and with three-dimensional electrodes, respectively, and has developed two photoelectrocatalytic reactors: slurry photoelectrocatalytic reactor [20] and three-dimensional electrode-slurry photocatalytic reactor [21,22], for the degradation of some pollutants in water. In the present study, a continuous flow three-dimensional electrode-packed bed photocatalytic reactor is also developed; this is an improvement on two photoelectrocatalytic reactors reported in our previous research works [20–22]. Reactive brilliant orange K-R (RBOKR) was used as a model compound to investigate the photoelectrochemical degradation feasibility of dyeing pollutants in a salt solution.

2. Experimental

2.1. Materials

RBOKR was a commercial grade reagent; the solutions were prepared with deionized water to the concentration of 0.5 mM. The formula of RBOKR is shown in Fig. 1. Except as indicated, NaCl was used as supporting electrolyte in the photoelectrocatalytic process at the concentration of $0.5 \, mol \, l^{-1}$. Titanium dioxide Degussa P25 is composed mainly of anatase (ca. 70%), having the shape of non-porous polyhedral particles with a size of ca. 30 nm mean size and a surface area of $50 \, m^2 \, g^{-1}$. Analytic grade quartz sand with particulate diameter of 2–4 mm was used as the supports of photocatalyst. The material prepared of quartz sand coated by TiO_2 was used both as the filler for the three-dimensional electrode and for the packed

bed photocatalyst in this photoelectrocatalytic reactor. The micropore titanium plate was used for electrodes after treatment with diluted sulfuric acid and then washing with deionized water twice. All other reagents were analytic grade.

2.2. Preparation of quartz sand-supported TiO_2

A 200 ml aqueous suspension containing 5 g TiO_2 was agitated for 4 h, and then sonicated for 30 min before coating on quartz sand. After quartz sand was carefully cleaned by sonication in deionized water, 500 g was immersed in the suspension solution for 30 min. The mixture was dried at 120 °C and then calcined 4 h in an oven at 450 °C. Loading, drying and calcining were repeated twice. After being washed with deionized water, the material was first dried at 120 °C and then weighted. The quantity of TiO_2 coating on quartz sand was about $0.0182 \, g \, g^{-1}$. The SEM micrographs of the coated material were obtained by a LEO1530VP microscope (LEO, Germany); a typical micrograph is presented in Fig. 2. It can be seen from the micrograph that TiO_2 was distributed uniformly on the supports, and that the average size is exactly the same as that of the original Degussa P25 TiO_2.

2.3. Photoelectrochemical reactor

The used set up is a continuous flow three-dimensional electrode-packed bed photocatalytic reactor. The reactor was based on the three-dimensional electrode-slurry photocatalytic reactor [21,22] and the slurry photoelectrocatalytic reactor [20], as reported in our previous researches. The reaction setup consisted of a 250 ml flow-through photoelectrocatalytic reactor connected to a 500 ml reservoir. As shown in Fig. 3, it consisted of an outer cylindrical Pyrex casing (i.d. = 60 mm; height = 300 mm) fitted with a gas distributor
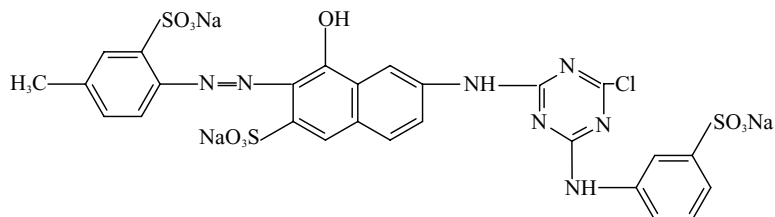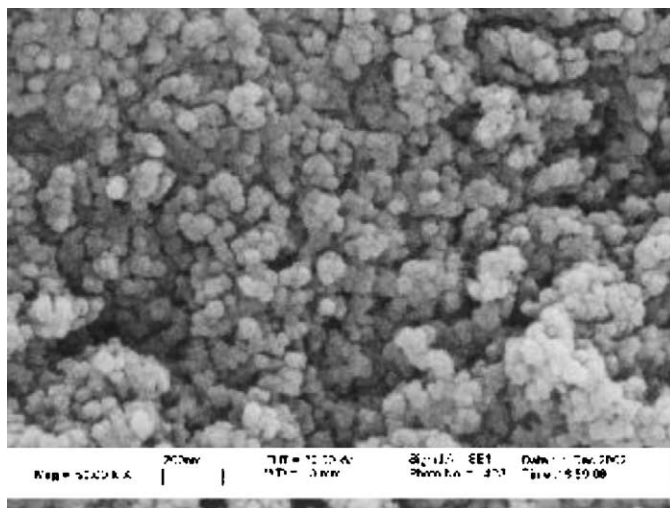

Fig. 1. Structure of RBOKR.

Fig. 2. A typical SEM micrograph of the quartz sand-supported TiO_2.

(porous titanium plate with a pore size of less than 40 μm) and a PVC base. A 500 W high-pressure mercury lamp was suspended vertically in a double-welled U-tube, through which 5.0 mm-thick cooling water flowed (800 ml min^{-1}) to maintain reaction isothermality. The quartz sand-supported TiO_2 was packed between the annulus of the inside quartz U-tube and the outer Pyrex cylinder, the thickness of the supports is 5.0 mm. The packed material was used as both for the photocatalyst of packed bed photocatalytic reactor and for the particle electrode of the three-dimensional electrode electrochemical reactor. That means the photoelectrocatalytic reactor is a packed-bed photocatalytic reactor coupled with a three-dimensional electrode electrochemical reactor. The compressed air was bubbled upwards through the porous titanium plate as a gas distributor on the bottom of reactor. Simultaneously, the titanium gas distributor was also used as the anode of the photoelectrochemical reactor while its cathode is a cirque made of porous titanium, located above the anode about 15 cm distant. External cell voltage was controlled by a WYK-305 potentiostat (Yangzhou, China). The reaction solution was recirculated through the system at a flow rate of ca. 190 ml min^{-1} using a peristaltic pump. Additionally, the exterior wall of the reactor was covered with a reflecting aluminum foil to improve the efficiency of UV utilization.
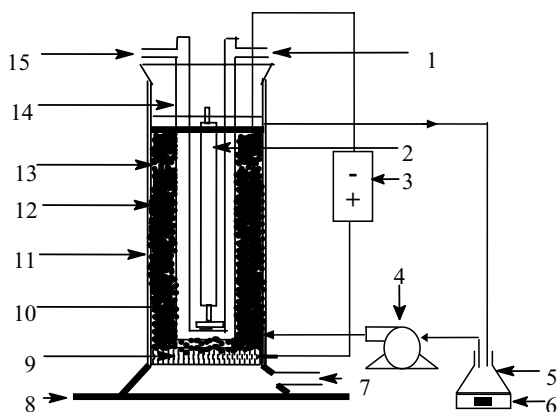

Fig. 3. Schematic of reactor setup. (1) Inlet of recycled water; (2) high pressure mercury lamp; (3) potentiostat; (4) pump; (5) reservoir; (6) magnetic stirrer; (7) inlet of compressed air; (8) base of reactor; (9) micropore titanium plate anode; (10) packed material; (11) aluminum foil; (12) outer Pyrex cylinder; (13) a porous titanium cirque cathode; (14) double-welled quartz U-tube; (15) outlet of recycled water.

2.4. Analysis

Millpore membrane (0.45 μm) was used to remove solid mass of the colloid solution before the UV analysis. The degradation of RBOKR in the reaction solution was monitored at the maximum absorption wavelength of 480 nm with a Helios Alpha UV-Vis spectrophotometer (Thermo Spectronic) and
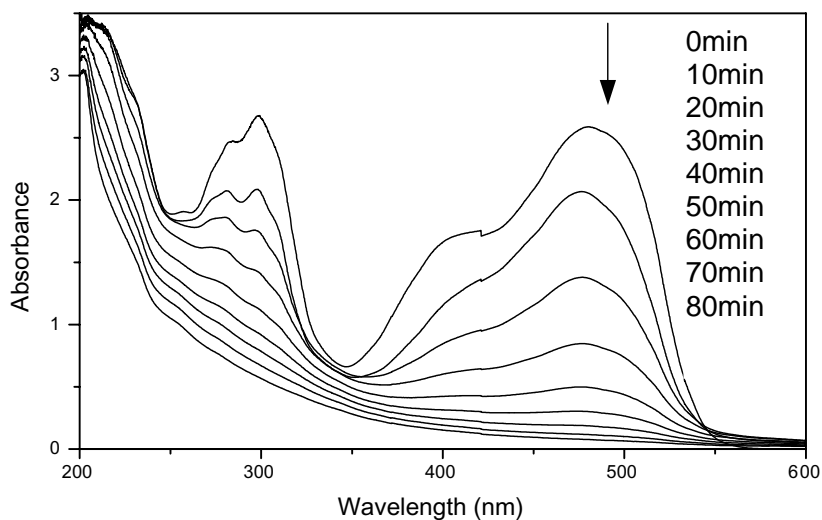
Fig. 4. Change of UV-Vis spectra of RBOKR degradation by photoelectrochemical process.

the total organic carbon reduction was measured with a Phoenix 8000 TOC analyzer.

2.5. Procedures

A 500.0 ml solution of RBOKR containing $0.5 \, \text{mol} \, l^{-1}$ NaCl was used to conduct the experiment. The solution was pumped through the photoelectrochemical reactor by a peristaltic pump at the flow of $190 \, \text{ml} \, \text{min}^{-1}$, and the residual solution was well stirred by a magnetic stirrer. The reaction was started when the dc power, illumination and compressed air supply were switched on. Except as indicated, general treating conditions were 30.0 V direct current cell voltage, 0.05 MPa airflow, $0.5 \, \text{mmol} \, l^{-1}$ RBOKR, natural pH value and $0.5 \, \text{mol} \, l^{-1}$ NaCl solution. Once the experiment started, samples were withdrawn from the reservoir at desired intervals for the analyses of the concentration of dye and the TOC.

3. Results and discussion

3.1. Investigation of decolorization and mineralization of RBOKR

The absorption spectra of RBOKR in the range of 200–600 nm were scanned; the absorption spectra

change in the photoelectrochemical process is shown in Fig. 4. From the figure it can be clearly seen that the RBOKR disappeared very quickly with the increase of reaction time. The other three processes, photocatalysis, electro-oxidation and adsorption, compared with photoelectrocatalysis process, were also carried out, and the comparison of removal efficiency of RBOKR is presented in Fig. 5. It is easy to see that only 9% RBOKR was removed by the adsorption of packed material within 60 min, which indicates that the photocatalysis and electro-oxidation process played
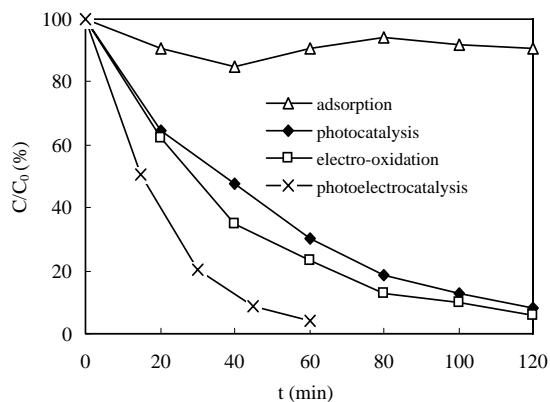

Fig. 5. Comparison of RBOKR removal by photoelectrocatalysis, photocatalysis, electro-oxidation and adsorption.

important roles in the decolorization of RBOKR. The decolorization efficiencies obtained by the two methods were 70 and 77%, respectively, while the decolorization efficiency by photoelectrocatalysis was much higher, up to 96%, within the identical time. The results indicated that the photocatalysis decolorization of RBOKR could be accelerated by combined use of three-dimensional electrode electrochemical technology in the reactor. This might be explained by supposing that external electric field reduced the chances of the recombination of the electron–hole pairs and thus the efficiency of photocatalysis was enhanced.

A similar conclusion can be drawn by comparison of the TOC reduction efficiency; the results are shown in Fig. 6. The isolated photocatalysis and electro-oxidation processes only led to TOC reduction of ca. 49 and 17% within 150 min, respectively, while the combined process obtained a higher TOC reduction, ca. 61%, than that in the single process. This showed that the combined use of three-dimensional electrode technology could significantly enhance not only the decolorization efficiency of RBOKR but also TOC reduction in photocatalytic process. Additionally, the reduction of TOC in the photocatalytic process was much higher than that in the electro-oxidation process, while the decolorization efficiency in the former process was lower than that in the latter process. This indicates that electro-oxidation may convert the dye to some intermediates quickly but the complete mineralization of them became very difficult.

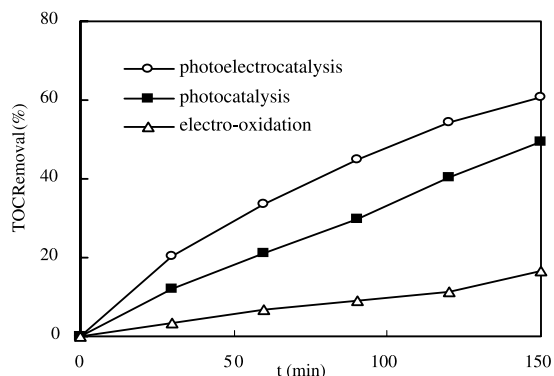From the above-mentioned, we are convinced that the dye could be degraded more efficiently by pho-toelectrochemical process than by photocatalytic oxidation or electrochemical oxidation alone, in terms of both decolorization and TOC removal. That means that photocatalytic process can be improved efficiently by the three-dimension electrode technology. The reaction mechanism for the three-dimension electrode-assisted photocatalytic degradation of the dye under higher electric field has been discussed in our previous publications [21,22]. The degradation mechanism can be carried out by many oxidation routines, such as anodic oxidation, the oxidation of electrogenerated H_2O_2 and $^\bullet OH$, the oxidation of photogenerated hole and $^\bullet OH$, and the photoelectrochemical synergic effect.

3.2. Effect of applied cell voltage

The effect of applied cell voltage on the degradation of RBOKR by photoelectrochemical process is shown in Fig. 7. It is obvious that the degradation rate of RBOKR increased dramatically as the applied cell voltage increased. For example, when the applied cell voltage increased from 2 to 30 V, the degradation rate constants of RBOKR increased rapidly from 0.0213 to 0.0539 min^{-1}, which means that the apparent rate constant of RBOKR degradation enhanced by 2.5-fold. The same phenomena were also observed in our previous reports [22]. It is explained by the fact that the external electric field could not only decrease the rate of recombination of electron-hole pairs, but could also improve the direct and/or indirect electro-oxidation reactions of anodes under higher applied cell voltages.
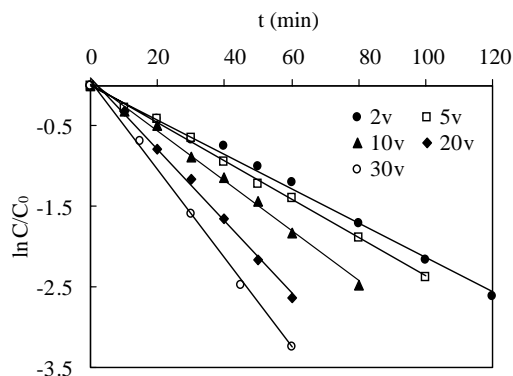

Fig. 6. Comparison of TOC removal in the degradation of RBOKR by photoelectrocatalysis, photocatalysis and electro-oxidation.

Fig. 7. Effect of applied cell voltage on the degradation of RBOKR.

3.3. Effect of Cl⁻ ion concentration

Inorganic anions such as Cl^-, SO_4^{2-} and PO_4^{3-} are frequently present in industrial wastewater. However, these species always inhibit the photocatalytic oxidation reaction of organic pollutants since they can compete for oxidizing radicals or the active sites of the TiO_2 catalyst [23–26]. So, how to overcome the detrimental effects of common inorganic anions on photocatalytic and photoelectrocatalytic reaction is of interest in practice. In the present experiment, NaCl was used as the supporting electrolyte of treated solution. Its effect on the photoelectrochemical oxidation of RBOKR is shown in Fig. 8. From this figure we can see that increasing the amount of NaCl can significantly enhance rather than inhibit the degradation of RBOKR. As compared with the result without addition of NaCl, the apparent rate constant of RBOKR degradation by photoelectrochemical process decreased slightly at lower concentration, but increased quickly when the chloride ion concentration was further increased. This would mean that at the lower Cl^- concentration the Cl^- took part in a competition for oxidizing radicals or the active sites of the catalyst, resulting in a scavenging effect on the photoelectrochemical degradation of RBOKR to some extent. However, with the increase of Cl^- concentration, the adsorption of Cl^- reaches an equilibrium; then the surplus free Cl^- as an electrolyte can enhance charge-transfer in the reactor as a supporting electrolyte, leading to the capture effect of photogenerated electron by external electric field. Moreover, increase
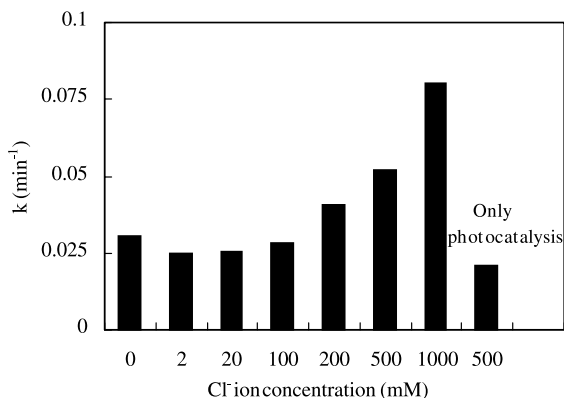
in electrolyte concentration can lead to a strong increase of degradation efficiency of RBOKR by direct and/or indirect electrochemical oxidation under high cell voltage. In addition, Cl_2, formed by direct or indirect electro-oxidation reaction of Cl^- in the reactor, can also assist the photocatalytic degradation of RBOKR. The comparison results of photocatalytic oxidation with photoelectrocatalytic oxidation at the same concentration of 500 mM NaCl were also given in Fig. 8. It is obvious that the degradation rate of photoelectrocatalysis was much faster than that of photocatalysis.

3.4. Effect of pH value

The pH value is an important parameter in the photocatalytic and photoelectrocatalytic process, because the species of the reaction compounds and its adsorption equilibrium on the TiO_2 depend on the pH values of reaction solution. Since the iso-electrical point of TiO_2 is at pH 4–6, the catalytic surface will be positively charged at more acidic pH values [27]. Moreover, the studied substrate, RBOKR, is a kind of anionic dye in the aqueous solution. At low pH value, RBOKR with negative charge can be adsorbed easily on the surface of TiO_2 with positive charges. However, beyond pH 6, the adsorption of the dye onto TiO_2 becomes difficult with increase in pH value due to the repellent effect of two species with negative charge. Therefore, it can be expected that more acidic pH values will be favorable to the photoelectrocatalytic degradation of RBOKR, which was further confirmed by the results shown in Fig. 9. We can see

Fig. 8. Effect of initial concentration of Cl^- ion on the degradation of RBOKR.
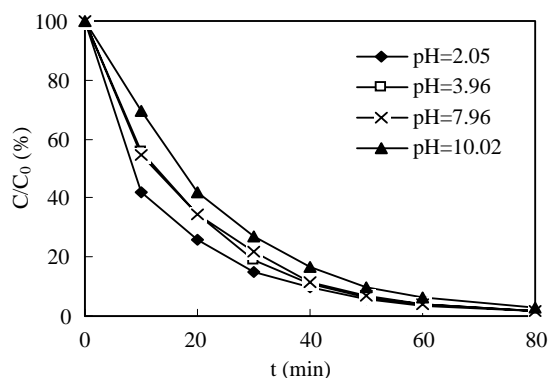

Fig. 9. Effect of pH value on the degradation of RBOKR.

from the figure that, at the initial stage of RBOKR oxidation, the reaction rate increased sharply with the decrease of pH value. For example, at 20 min, 74% of RBOKR was removed at pH 2.05 while only 58% of RBOKR was removed at pH 10.02.

3.5. Effect of airflow

In a photocatalytical process, oxygen is necessary to form superoxide radical anions that will further generate other active radicals to promote the degradation reaction [17]. Furthermore, the distribution of the intermediates is different in the presence and absence of oxygen [28]. Although the use of anodic bias obviates the need of oxygen as an electron acceptor in photoelectrochemical catalysis, the presence of molecular oxygen affects both the degradation rate and the degradation pathways of organic pollutants [6,18]. As stated above, the compressed air was sparged into the reactor from the bottom of the reactor in the run. Thus, the photoelectrocatalytic oxidation of RBOKR was conducted at different airflow values. The results are shown in Fig. 10. Obviously, the airflow plays an important role in the photoelectrochemical process. When no air was sparged, the reaction rate was relatively slow. However, the reaction rate increased significantly with the increase of airflow. From the figure, we can see that, when the airflow continues to increase from 0.05 to 0.075 MPa, the photoelectrocatalytic reaction rate changed slightly. This is because further increasing the airflow, the charge separation, and the oxygen dissolving will reach an equilibrium, resulting in a slight change of reaction rate.
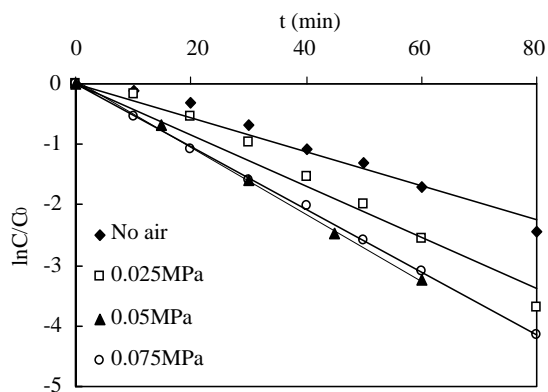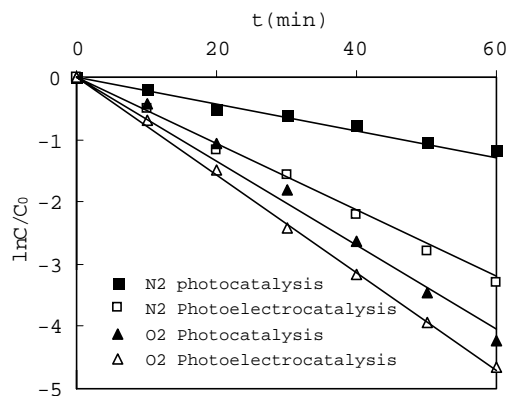

Fig. 11. Effect of various sparged gases on the degradation of RBOKR.

In the present study, pure nitrogen and oxygen were sparged into the reactor in order to understand their influence on the photocatalytic and photoelectrochemical oxidation of RBOKR, respectively; the results are shown in Fig. 11. It is clear that the reaction rates in N_2-purged photocatalytic and photoelectrocatalytic process, respectively, were much smaller than that of oxygen. At 20 min, 40% of RBOKR was degraded in the N_2-sparged gas while 65% of RBOKR was degraded in the O_2-sparged gas in the photocatalytic process. However, in the case of the photoelectrocatalytic process, 31% of RBOKR also remained in the solution in N_2-sparged, while 22% of RBOKR remained in the solution in O_2-sparged process. This enhancement effect of oxygen on the photocatalytic and photoelectrocatalytic process is due to the capturing effect of photogenerated electrons by dissolving oxygen, reducing the recombination of electrons and holes. Thus, it can be concluded that the oxygen is very important for the photoelectrochemical oxidation of RBOKR under our experimental conditions. The results were in agreement with those obtained by Kim and Aderson [14] and in our previous research [20].

3.6. Effect of initial concentration of RBOKR

Fig. 12 shows the profiles of photoelectrochemical degradation of RBOKR at various initial concentrations of the dye by changing the concentration from 0.25 to 1 mmol l^{-1}. It can be seen that the reaction rate decreased sharply with the increase of the initial

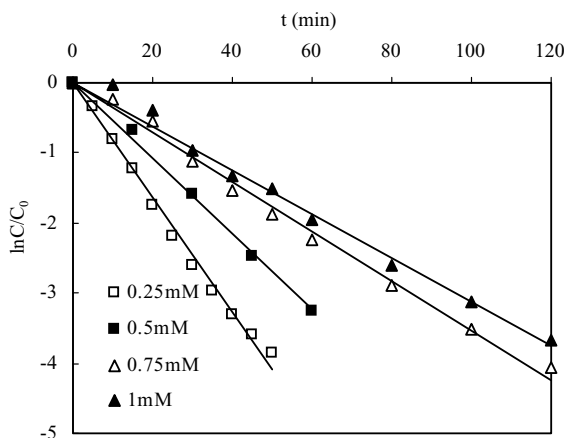Fig. 10. Effect of airflow on the degradation of RBOKR.

Fig. 12. Effect of initial concentration of RBOKR on the degradation rate.

concentration of RBOKR. Moreover, the degradation of RBOKR at various initial dye concentrations can be well fitted with the first order kinetic equation; this profile was also shown in the inset of Fig. 12. The decreasing trend of decolorization efficiencies at higher dye concentrations may be due to the combined effects of increased dye concentration and decreased transparency of dye solution. Similar observations were reported in the single photocatalytic process [29].

4. Conclusions

A new continuous flow photoelectrocatalytic reactor was reported to investigate the feasibility of photoelectrocatalytic degradation of a reactive dye in a salt solution. The experiments demonstrated that the photoelectrochemical process had higher efficiency in the decolorization and TOC removal of RBOKR than that in the efficiencies in cases of conventional photocatalytic and electro-oxidation used alone. That is, the photocatalytic degradation of RBOKR in a salt solution can be substantially improved by the three-dimensional electrode technology. And it is interesting to find that an obvious enhancement effect rather a scavenging effect on the photoelectrocatalytic degradation of RBOKR existed in the photoelectrocatalytic reactor in the presence of a high concentration of chloride ion.

References

[1] R. Camp, P.E. Sturrock, Wat. Res. 24 (1990) 1275.
[2] K.T. Fletcher, J. Text. Inst. 89 (1998) 72.
[3] R.J. Davis, J.L. Gainer, G. O'Neal, I. Wu, Wat. Environ. Res. 66 (1994) 50.
[4] C. Hachem, F. Bocquillon, O. Zahraa, M. Bouchy, Dyes and Pigments 49 (2001) 117.
[5] F. Kiriakidou, D.I. Kondarides, X.E. Verykios, Catal. Today 54 (1999) 119.
[6] K. Vinodgopal, E.E. Wynkoop, P.V. Kamat, Environ. Sci. Technol. 30 (1996) 1660.
[7] A.K. Ray, Catal. Today 44 (1998) 375.
[8] K. Takeda, K. Fujiwara, Wat. Res. 30 (1996) 323.
[9] O.A. Ileperuma, E.G. Verwey, J.T.G. Overbeek, Appl. Catal. 62 (1990) L1.
[10] J. Matos, J. Laine, J.M. Herrmann, App. Catal. B: Environ. 18 (1998) 281.
[11] S.A. Walker, P.A. Christensen, K.E. Shaw, J. Electroanal. Chem. 393 (1995) 137.
[12] I.M. Butterfield, P.A. Christensen, A. Hamnett, K.E. Shaw, G.M. Walker, S.A. Walker, C.R. Howarth, J. Appl. Electrochem. 27 (1997) 385.
[13] R.J. Candal, W.A. Zeltner, M.A. Anderson, Environ. Sci. Technol. 34 (2000) 3443.
[14] D.H. Kim, M.A. Anderson, Environ. Sci. Technol. 28 (1994) 479.
[15] H. Liu, S. Cheng, M. Wu, H. Wu, J. Zhang, W. Li, C. Cao, J. Phys. Chem. 104A (2000) 7016.
[16] R. Pelegrini, P. Peralta-Zamora, A.R. Andrade, J. Reyes, N. Duran, Appl. Catal. B: Environ. 22 (1999) 83.
[17] K. Vinodgopal, S. Hotchandani, P.V. Kamat, J. Phys. Chem. 97 (1993) 9040.
[18] K. Vinodgopal, U. Stafford, K.A. Gray, P.V. Kamat, J. Phys. Chem. 98 (1994) 6797.
[19] X.Z. Li, F.B. Li, C.M. Fan, Y.P. Sun, Wat. Res. 36 (2002) 2215.
[20] T.C. An, Y. Xiong, G.Y. Li, C.H. Zha, X.H. Zhu, J. Photochem. Photobiol. 152 (2002) 155.
[21] T.C. An, X.H. Zhu, Y. Xiong, J. Environ. Sci. Health 36A (2001) 1796.
[22] T.C. An, X.H. Zhu, Y. Xiong, Chemosphere 46 (2002) 897.

[23] M. Abdullah, G.K. Low, R.W. Matthews, J. Phys. Chem. 94 (1990) 6820.

[24] D.D. Dionysiou, M.T. Suidan, E. Bekou, I. Baudin, J.M. Laine, Appl. Catal. B: Environ. 26 (2000) 153.

[25] A. Piscopo, D. Robert, J.V. Weber, Appl. Catal. B: Environ. 35 (2001) 117.

[26] K.H. Wang, Y.H. Hsieh, C.H. Wu, C.Y. Chang, Chemosphere 40 (2000) 389.

[27] D.H. Kim, M.A. Anderson, J. Photochem. Photobiol. A: Chem. 94 (1996) 221.

[28] M.S. Dieckmann, A.G. Kimberly, Wat. Res. 30 (1996) 1169.

[29] I. Arslan, I.A. Balcioglu, D.W. Bahnemann, Dyes and Pigments 47 (2000) 207.